Inhibition of endoplasmic reticulum stress and activation of autophagy-protect intestinal and renal tissues from western diet-induced dysbiosis and abrogate inflammatory response to LPS: role of vitamin E

A.M. Shamseldeen[1], M. Hamzawy[1], N.A. Mahmoud[1], L. Rashed[2], S.S. Kamar[3], I.A. Harb[4] and N. Sharawy[1]

[1]Department of Physiology, Faculty of Medicine, Cairo University, Cairo, Egypt; [2]Department of Biochemistry, Faculty of Medicine, Cairo University, Cairo, Egypt; [3]Department of histology, Faculty of Medicine, Cairo University, Cairo, Egypt; [4]Department of Medical Pharmacology, Faculty of Medicine, Cairo University, Cairo, Egypt

Received November 25, 2020 – Accepted March 22, 2021

Diet pattern is an emerging risk factor for renal disease. The mechanism by which high-fat high fructose (western) diet mediates renal injury is not yet fully understood. The objective of the present study was to investigate the relationship between endoplasmic reticulum (ER) stress and autophagy in the development of renal impairment and aggravation of the inflammatory response. Eighty male rats were randomly divided into four groups as follows: a standard diet-fed (ConD), a high-fat high fructose diet fed (HFHF-V), ConD fed and orally supplemented with vitamin E (ConD-E), and HFHF fed and orally supplemented vitamin E (HFHF-E). After 12 weeks, either lipopolysaccharide (LPS) or saline was injected. We found that upregulation of endoplasmic reticulum stress-related proteins rendered the cells susceptible to injury induced by dysbiosis and microbiota-derived metabolites. A downregulation of autophagy and upregulation of caspase-12 resulted in the loss of intestinal integrity and renal tubular injury. Maintained ER stress also increased the inflammatory response to LPS. In contrast, vitamin E effectively ameliorated ER stress and promoted autophagy to protect intestinal and renal tissues. Our results provide insight into the influences of sustained ER stress activation and autophagy inhibition on the development of renal injury, which may contribute also to the enhanced inflammatory response.

Renal diseases continue to carry a high burden of morbidity and mortality. Western diet (WD), an energy-dense high-fat and high-sugar diet, has been recently recognized to be a risk factor for the development of renal disease. In recent years, the dysregulation of gut microbiota and stimulation of inflammation pathways have been implicated in the development of the renal disease (1), however, there is little information available on the molecular mechanism behind this alteration.

The endoplasmic reticulum (ER) is a multifunctional organelle that controls lipid biogenesis, protein folding, and calcium homeostasis. When ER is subjected to harmful stimuli, the ER stress response is activated, with subsequent accumulation of unfolded proteins in the ER lumen. Several pathways linking ER stress to cell survival, inflammation, and autophagy. ER stress activates three transmembrane proteins: inositol-requiring protein 1 (IRE1), PKR [double-stranded-RNA-

Key words; apoptosis; endoplasmic reticulum stress; autophagy; NFκB; kidney disease

Corresponding Author:
Dr Nivin Sharawy,
Kasr El-Aini, Cairo University, AlSaray Street,
11562 Cairo, Egypt
Tel.: +202 01122433182
fax: +202 23628246
e-mail: nivin.sharawi@kasralainy.edu.eg

0393-974X (2021)

dependent protein kinase]-like ER kinase (PERK), and activating transcription factor 6 (ATF6), which modulate the expressions of nuclear target genes, including activating transcriptional factor 4 (ATF4), transcriptional factor C/EBP homologous protein (CHOP) and X-box binding protein-1 (XBP1). Recent studies have suggested that numerous diseases are caused by the abnormal expression of ATF4, ATF6, CHOP, and XBP1 in ER stress (2-3). As severe ER stress conditions continue, the apoptosis signaling pathways were reported to be initiated via induction of caspase 12 (4). Furthermore, ER stress intersects with various inflammatory signaling pathways, such as nuclear factor Kappa B (NFκB) signaling, to regulate cytokine production (5-7).

Autophagy is the process by which cytoplasmic components are engulfed into intracellular vesicles (autophagosomes) that fuse with lysosomes to be degraded. Growing evidence supports the idea that autophagy is important in ER quality control. Studies have also strongly indicated that autophagy could be triggered by unfolded proteins to remove damaged endoplasmic reticulum (reticulophagy) (8-9). Furthermore, suppression of autophagy was found to render hepatocytes vulnerable to ER stress (10-11). However, there is no conclusive demonstration of the interplay between ER stress and autophagy in WD-induced renal injury.

Vitamin E has been shown to exert anti-inflammatory effects in different chronic diseases. Accumulating evidence demonstrated the role of vitamin E in determining cell viability under different stress conditions (12, 13). Only a few controversial studies are available on the effect of vitamin E on ER stress. Vitamin E was found to induce ER stress in cancer cells (12), however, ER stress was found to be reduced by vitamin E during atherosclerosis (14). The effects of vitamin E on the various markers for ER stress and autophagy in WD-induced renal impairment are yet to be identified.

In this study, we investigated the effects of high-fat high fructose (HFHF) on the expression of ER stress and autophagy markers in intestinal and renal tissues. We also elucidate the involvement of microbiota-derived metabolites [short-chain fatty acid (SCFA)] in the regulation of renal response to HFHF and LPS. Furthermore, we aimed to determine whether vitamin E supplementation would induce autophagy and ameliorate ER stress to protect against renal injury.

MATERIALS AND METHODS

Experimental protocol

The animal protocol was approved by the research ethics committee at the Faculty of Medicine, Cairo University, and the Institutional Animal Care and use committee, Cairo University (protocol number CU III s5617). Animals were treated following Canadian Council on Animal Care (CCAC) guidelines. Male Wister albino rats were purchased from the animal house of Kasr El Aini, Faculty of Medicine, Cairo University, and housed in individual cages maintained in a temperature-controlled environment, with a 12-h light/dark cycle and allowed ad libitum access to diets and drinking water.

High fat-high fructose (HFHF) diet, containing (gm %): Protein 24; Carbohydrate 41and Fat 24 (Product #D12451; Research Diets, New Brunswick, USA) with an additional 30% of fructose in water was used. The control diet consisted of (gm %): Protein 19.2; Carbohydrate 67.3 and Fat 4.3 (Product #D12450B; Research Diets, New Brunswick, USA).

The rats were randomly fed on ConD or HFHF-diet and were further divided into four subgroups: i. ConD-E: rats were fed a ConD for 3 months in concomitant with the administration of vitamin E dissolved in palm oil orally in a dose of 250 mg/kg/day (15, 16); ii. ConD-V: rats were fed a ConD for 3 months in concomitant with the administration of equal volume of palm oil orally daily; iii. HFHF–E: rats were fed an HFHF for 3 months in concomitant with the administration of vitamin E; iv. HFHF-V: rats were fed an HFHF diet for 3 months in concomitant with the administration of an equal volume of palm oil. After 12 weeks, the rats were given intraperitoneal bolus injections of either 10 mg/kg body weight lipopolysaccharide (LPS) (Sigma Chemical, St Louis, MO) (17) (18) diluted in saline (ConD-LPS, HFHF-LPS, ConD-LPS-E, HFHF-LPS-E) or equal volumes of saline (ConD-V, ConD-E, HFHF-V, HFHF-E).

Animal weight, food and water consumption were measured every other day during the experiment. At the

end of the study, urine, faeces, and blood of each rat were collected, and serum was obtained by centrifugation of blood at 1500× g for 10 min and stored at −80°C until further analysis. The rats were sacrificed by decapitation 24 hours after LPS injection. Intestinal and renal tissues were rapidly removed and stored at −80°C until analysis.

Quantification of firmicutes and bacteroides

Bacterial DNA was amplified based on the amplification of genomic DNA coding 16S ribosomal RNA. Faecal microbiological DNA was analyzed using QIAamp DNA Mini Kit (Qiagen, Valencia, USA). We used the specific forward and reverse primers for Firmicutes phylum and Bacteroidetes phylum: Bacteroidetes (F: 5'-CATGTGGTTTAATTCGATGAT-3'; R: 5'-AGCTGACGACAACCATGC AG-3') and Firmicutes (F: 5'-ATGTGGTTTAATTCGAAGCA-3'; R: 5'-AGCTGACGA CAACCATGCAC-3'). Gut microbiota was quantitatively analyzed using SYBR Green quantitative PCR.

Renal function analysis

Creatinine and blood urea nitrogen (BUN) levels were detected using the conventional colorimetric QuantiChrom TM assay (BioAssay Systems, USA) to measure the absorbency of colour wave, as previously described (18) (19). The Creatinine clearance (CCr) was determined using the following equation: CCr (ml/min/kg of body weight) = [urinary Cr (mg/dl) × urinary volume (mg)/serum Cr (ml/dl)] × [1000/body weight (g)] × [1/1440 (min)].

The expressions of urinary neutrophil gelatinase-associated lipocalin (NGAL) in different groups of rats were quantified using Enzyme-linked immunosorbent assay (ELISA) kits (MyBioSource.com, San Diego, California, USA), as previously reported (20). The mean absorbance was measured spectrophotometrically at 450nm in a microplate reader

Serum LPS and SCFA analysis

Quantitative ELISA was employed to measure the concentration of LPS in the serum. Antibody specific for LPS (CUSABIO Technology LLC; Houston, USA) was pre-coated onto a microplate. 100 µl standard as well as samples were added to the corresponding well. Both sample and buffer were incubated together with LPS-Horseradish Peroxidase (HRP) conjugate in a pre-coated plate for 1 h. After the incubation, the wells were washed and incubated with a substrate for HRP enzyme. The intensity of the developed color was detected at 450 nm on a microplate reader.

The circulating SCFA analysis was performed using gas chromatography-mass spectrometry analysis as previously reported (21, 22). Briefly, derivatized samples were injected in a gas chromatograph (Agilent Technologies) coupled to a mass spectrometer detector. The analysis was performed using a linear temperature gradient at 65°C up to 280°C for 5 min. The injector and transfer line temperatures were kept at 250°C. Serum SCFA was quantified by comparing the spectrum with the internal standard.

Analysis of nuclear *factor-kappa B (NF-κB) protein expression in the intestinal and renal tissues*

The concentration of NF-kB p65 in intestinal and renal tissues supernatants was evaluated using the rat NF-kB p65 (ELISA) kit (MyBioSource.com, San Diego, California, USA). The intensity of color was spectrophotometrically detected at 450 nm using a 96-well plate reader. The NF-κB concentration was estimated by comparing the optical densities of the samples with the standard curve.

Quantitative Real-Time PCR analysis

Total cellular RNA was isolated from intestinal and renal tissues using the Qiagen tissue extraction kit (Qiagen, USA) according to the manufacturer's instructions. 0.5–2 µg of extracted RNA was inversely transcribed into cDNA using a high-capacity cDNA reverse transcription kit. Real-time qPCR amplification and analysis were performed using an Applied Biosystem with software version 3.1 (StepOne™, USA). Gene expression was normalized to the internal standard basic transcription beta-actin. The following primer pairs were used for amplification: occludin, ZO-1, TLR4, caspase-12, Vamp8, LAMP, ATF 4, ATF 6, CHOP, XBP1, Beta-actin (Table I).

mTOR, Beclin-1, and LC3 protein analysis by Western blot

Western blot was used to quantify autophagy biomarkers in the intestinal and renal tissues. Renal and intestinal tissues were lysed in RIPA buffer (Marhham, Ontario L3R 8T4, Canada). Thereafter, supernatant fluids were collected to measure the protein levels, using

Bradford Protein Assay Kit (BIO BASIC INC. Markham Ontario L3R 8T4 Canada). 5-20 ug protein concentration of each sample was loaded with an equal volume of 2x Laemmli sample buffer, and the mixture was boiled at 95°C for 5 min to ensure denaturation of protein before polyacrylamide gel electrophoresis. The samples were transferred onto a PVDF membrane followed by the addition of primary antibodies against mTOR (1:1000; Thermofisher, USA); beclin-1 (1:1000; Thermofisher, USA), and LC3 (1:1000; Thermofisher, USA).

Table I. *Sequences of primers used in real-time polymerase chain reaction (Real-time PCR)*

Gene	**Primer sequences (5′-3′)**	
occludin	Forward	5’-GCTATGAAACCGACTACACGACA-3’
	Reverse	5’-ACTCTCCAGCAACCAGCATCT-3’
ZO-1	Forward	5’-AGGCTATTTCCAGCGTTTTGA-3’
	Reverse	5’-AATCCTGGTGGTGGTACTTGC-3’
TLR4	Forward	5′-TCATCCAGGAAGGCTTCCA-3′
	Reverse	5′-GCTGCCTCAG CAAGGACTTCT-3′
caspase-12	Forward	5′-TTCATTATTCAGGCCTGCCGAGG -3′
	Reverse	5′ TTCTGACAGGCCATGTCATCCTCA-3′
Vamp8	Forward	5′-CCCTCTCCTGTCCTCCTCCA-3′
	Reverse	5′-TCTCCTCCCAGGGGATCAAG-3′
LAMP	Forward	5′-TGCTGGCTACCATGGGGCTG-3′
	Reverse	5′-GCAGCTGC CTGTGGAGTGAGT-3′
ATF 4	Forward	5′-GCCGGTTTAAGTTGTGTGCT-3′
	Reverse	5′-CTGGATTCGAGGAATGTTGCT-3′
ATF 6	Forward	5′-GATGCAGCACATGAGGCTTA-3′
	Reverse	5′-CAGGAACGTGCTGAGTTGAA-3′
CHOP	Forward	5′-GAAAGCAGAAACCGGTCCAAT-3′
	Reverse	5′-GGATGAGATATAGGTGCCCCC-3′
XBP1	Forward	5′-AAACAGAGTAGCAGCGCAGACTGC-3′
	Reverse	5′-GGATCTCTAAAACTAGAGGCTTGGTG-3′
BETA ACTIN	Forward	5′-AGGCATCCTCACCCTGAAGTA-3′
	Reverse	5′CACACG-CAGCTCATTGTAGA-3′

Chemiluminescent substrate (Clarity™ Western ECL substrate - BIO-RAD, USA cat#170-5060) was used to the blot according to the manufacturer's recommendation.

Histological analysis

The kidneys and jejuna tissues of each rat were dissected, fixed in formaldehyde, and embedded in paraffin. Sections of 6 μm thickness were obtained and stained with hematoxylin and eosin (H&E). The morphological changes were analyzed using a light microscope equipped with (Leica Qwin 500 C; Cambridge) image analysis software.

Histological changes in renal tissue were evaluated at 10 randomly selected fields and scored as illustrated in a previous study (23). The tubular injury was defined as cellular degeneration and vacuolization, tubular dilatation, and cast formation. According to the aforementioned criteria, 0 = normal renal architecture, 1 = renal damage involved less than 25% of the tubular area, 2 = renal damage between 25% and 50% of the tubular area, 3 = renal damage between 50% and 75% of the tubular area, and 4 = renal damage between 75% and 100% of the tubular area. Jejuna samples were analyzed for the inflammatory cell infiltration, epithelial damage, and mucosal architecture, as illustrated previously (24) and summarized in Table II.

Statistical analysis

The data were analyzed using Graph Pad Prism software (version 5.0; San Diego, California USA). One-way ANOVA plus Newman-Keuls's post hoc multiple comparison tests were used to analyze differences between the groups. Two-way ANOVAs (subject factors: Time and diet) were used to analyze data from the total water and food consumption. Pearson's correlation coefficient was used to estimate the relationship between variables. In this study, the value of r was used to represent the strength of the correlationship. In all cases, $\mathbf{P}<0.05$ was taken to indicate significance. All data are expressed as mean ± SEM.

RESULTS

Bodyweight and food and water consumption

The results showed that the body weight gain was significantly increased ($\mathbf{P} < 0.05$) in all HFHF fed rats when compared to their respective counterparts on control diets. There was no significant difference in average fluid intake yield by diet ($F=5.9$, $P<0.0001$) and time ($F=4.9$, $P<0.0001$), however, diet ($F=4.4$, $P<0.0001$), but not time ($F=0.18$, $P=0.99$), had a significant effect on food consumption, and no significance was found in the interaction between both factors (Fig. 1).

Table II. *Intestinal injury scoring system*

Findings	Definition	Scoring
Inflammatory infiltrates	Minimal (less than 10%)	1
	Mild (10-25%)	2
	Moderate (26-50%)	3
	Marked (more than 51%)	4
Epithelial damage	Focal erosions	1
	Multiple erosions	2
	Villous denudation	3
Mucosal architecture:		
- Villous shortening	Mild: villous/crypt ratio of 2:1 to 3:1.	2
	Moderate: villous/crypt ratio of 1:1 to 2:1.	
	Non-parallel crypts, variable crypt diameters	3
- Irregular crypts		4

HFHF **acted synergistically with LPS to** *increase Firmicutes and intestinal injury score and reduce occludin and vitamin E reversed the effects of HFHF and LPS*

HFHF-fed rats (with and without LPS) and ConD-LPS elicited a significant increase ($P < 0.05$) in Firmicutes and a significant decrease ($P < 0.05$) in Bacteroides, compared with rats on the control diet and not subjected to LPS (ConD-V and ConD-E). Small intestinal gene expressions revealed that HFHF, HFHF-LPS, and ConD-LPS rats had lower ($P < 0.05$) levels of occludin and ZO-1 compared with ConD-V and ConD-E rats. Furthermore, rats fed HFHF and challenged with LPS showed a significant increase ($P < 0.05$) in Firmicutes and a decrease in occludin, when compared to HFHF-V and ConD-LPS groups (Fig. 2 A-D). Moreover, intestinal histological score and caspase-12 were significantly increased ($P < 0.05$) in rats receiving HFHF-LPS than other rats receiving either HFHF or LPS. The rats of control groups (ConD-V and ConD-E) showed no intestinal injury (Fig. 2 E-G).

Compared with the vehicle-treated groups (HFHF-V, HFHF-LPS and ConD-LPS), Firmicutes, caspase-12, and intestinal injury scores were significantly decreased ($P < 0.05$) in the vitamin E-treated groups (HFHF-E, HFHF-LPS-E, and ConD-LPS-E). Moreover, all vitamin E-treated rats (HFHF-E, HFHF-LPS-E, and ConD-LPS-E) showed significantly increased ($P < 0.05$) gene expressions of occludin and ZO-1 (Fig. 2).

HFHF **acted synergistically with LPS to** *increase serum LPS and SCFA and promote renal injury and vitamin E reversed the effects of HFHF and LPS*

We assumed that the increased serum LPS and SCFA, produced by gut microbiota, would

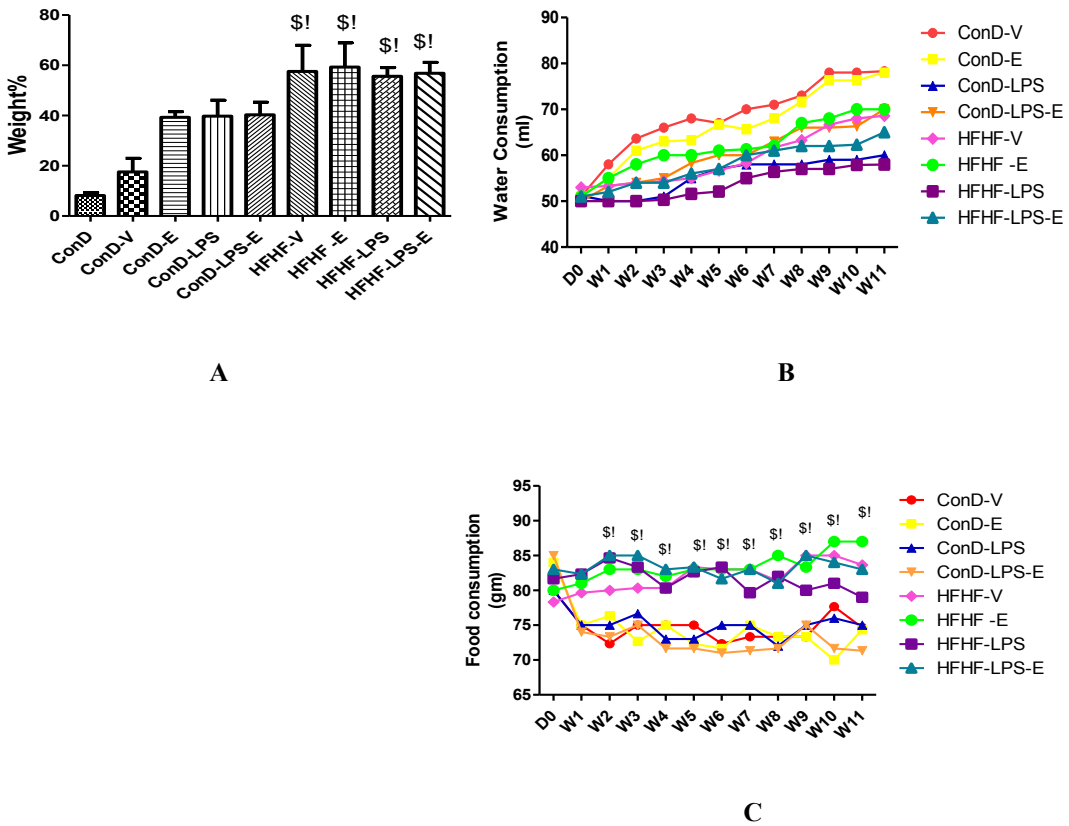

A **B** **C**

Fig. 1. *Evaluation of body weight gain and food and water consumption of rats on different dietary regimens and challenged with lipopolysaccharide (LPS). Data are expressed as the percentage (%) of body weight gain relative to the initial body weight. ConD: control diet; HFHF: High-fat-High-Fructose diets; LPS: lipopolysaccharide; E: vitamin E; V: vehicle. Data are expressed as mean ± SEM. $ p<0.05 vs ConD-V, ! p<0.05 vs ConD-E.*

enhance the development of acute kidney injury after endotoxin injection. To validate this, we examined the relationship of serum LPS and SCFA to the development of renal impairment. Detailed analysis of kidney function and structure revealed a significant increase (**P** < 0.05) in renal caspase-12 and renal impairment in ConD-LPS as well as untreated HFHF feeding rats (HFHF-V and HFHF-LPS). In the renal morphological analysis, the bowman's space in the rats on an HFHF and/or LPS tended to be dilated. Furthermore, tubular hyaline casts, apoptotic degeneration, and inflammatory cell infiltrations were observed in LPS, HFHF as well as HFHF-LPS groups (Table III, Fig. 3).

Concomitantly, serum levels of LPS and SCFA were significantly increased (**P** < 0.05) in untreated HFHF feeding rats (with and without LPS) and ConD-LPS, when compared to rats on the control diet (Conn-V and ConD-E). Moreover, HFHF acted synergistically to significantly increase (**P** < 0.05) serum LPS and SCFA, and to significantly enhance (**P** < 0.05) LPS induced renal injury. Compared to untreated rats (HFHF-V, HFHF-LPS, and ConD-LPS), rats subjected to HFHF and/or LPS and treated with Vitamin E showed a significant reduction (**P** < 0.05) in renal injury as well as serum levels of SCFA and LPS, as shown in Fig. 3. Increased levels of SCFA and LPS were found significantly correlated

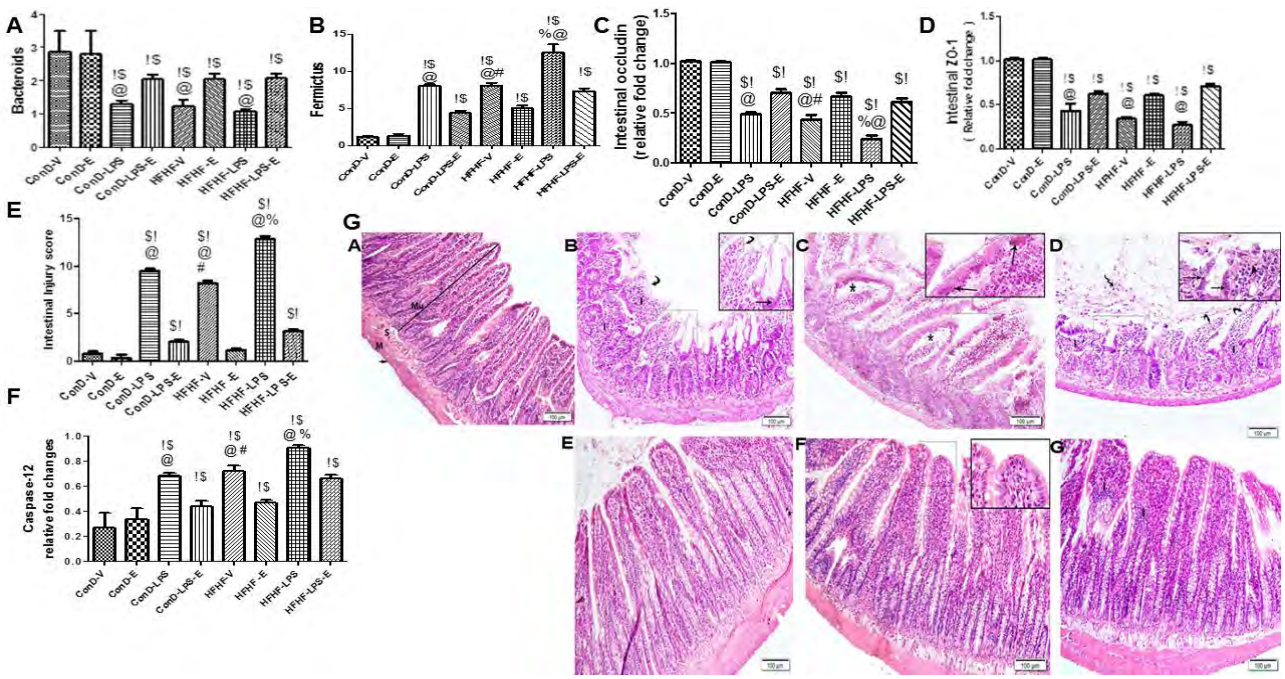

Fig. 2. *A high-fat high fructose diet modified the microbiota composition and enhanced endotoxin-induced intestinal injury and vitamin E reversed the effects. Alterations in the intestinal Bacteroides (A) and Firmicutes (B) were associated with modulations of the intestinal occludin (C) and ZO-1. (D) mRNA expression levels. E, F) Quantifications of intestinal injury and caspase-12 mRNA level. G) Representative hematoxylin and eosin (H&E) stained images of intestinal tissue at 100 × and 400 x magnification for Control group (A) showing the normal structure of intestinal layers; ConD-LPS group (B) with distortion of the villi with the sloughed epithelium of some parts (curved arrow)and the inflammatory cells infiltration (I), HFHF-V(C) showing brooding and distortion of the villi and oedema (star) in lamina propria, HFHF-LPS (D) with substantial distortion of most of the villi with obvious denudation and the inflammatory cells infiltration in the intestinal mucosa (I) and the lumen of the intestine (wavy arrow). Vitamin E preserved the morphological structure of the intestinal mucosa, submucosa, musculosa, and serosa in ConD-LPS-E (E) and HFHF-E (F). Some inflammatory infiltrations (I) were noted in some villi in HFHF-LPS-E (G). ConD: control diet; HFHF: High-fat-High-Fructose diet; LPS: lipopolysaccharide; E: vitamin E; V: vehicle. Data are expressed as mean ± SEM. $ p<0.05 vs ConD-V, ! p<0.05 vs ConD-E, @ p<0.05 vs respective vitamin E treated group, % p<0.05 vs ConD-LPS, # p<0.05 vs HFHF-LPS.*

with renal damage. Creatinine, NGAL, and renal injury score values were positively and significantly correlated with serum LPS and SCFA levels (Table IV).

HFHF **acted synergistically with LPS to** *increase TLR4 and NFKB expressions in intestinal and renal tissues and vitamin E reversed the effects of HFHF and LPS*

In intestinal and renal tissues, the data revealed a significant increase (**P** < 0.05) of TLR4 and NF-κB expressions in ConD-LPS, HFHF, and HFHF-LPS. Additionally, HFHF combined with LPS significantly aggravated (**P** < 0.05) the effect of LPS or HFHF on TLR4 and NFKB expressions. In contrast, vitamin E significantly reduced (**P** < 0.05) TLR4 and NF-κB levels compared with untreated groups (HFHF-V, HFHF-LPS, and ConD-LPS) (Fig. 4).

HFHF **acted synergistically with LPS to promote ER stress** *in intestinal and renal tissues and vitamin E reversed the effects of HFHF and LPS*

ConD-LPS, HFHF, and HFHF-LPS were found to induce the activation of ER stress in intestinal as well as renal tissues. As shown in Fig. 5, the expression levels of the ER stress-related proteins ATF 4, ATF6, CHOP, and XBP1 were all significantly enhanced ($p<0.05$) after LPS or HFHF compared with control groups (ConD-V and ConD-E), with the highest increase observed in HFHF-LPS. However, vitamin E significantly decreased ($p<0.05$) the ER stress both

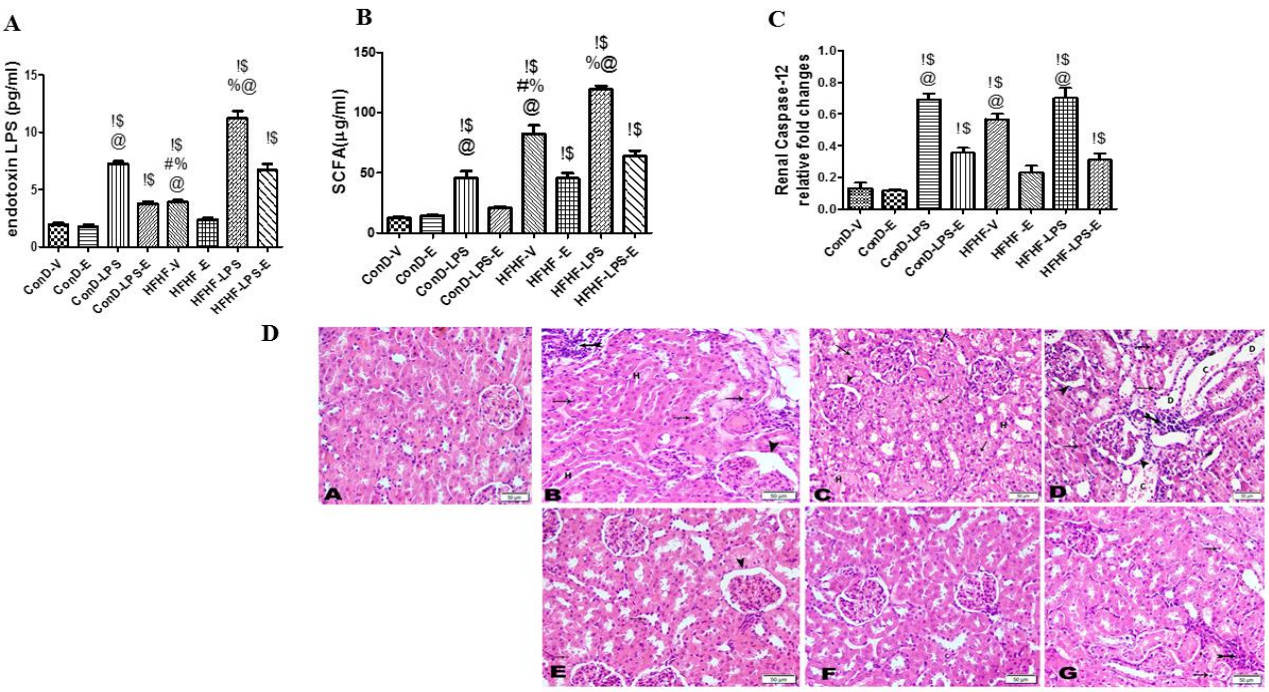

Fig. 3. *The relationship between serum short-chain fatty acids (SCFA) and lipopolysaccharide (LPS) and the degree of renal injury. A, B) Quantifications of LPS and SCFA in the serum. E) Quantifications of renal caspase-12 mRNA level. D) Representative photomicrographs for hematoxylin and eosin staining (at 200×magnification) of kidney sections of rats fed a control diet (ConD) (A), ConD and subjected to LPS (B), high-fat high fructose (HFHF) diets (C), and HFHF diet and subjected to LPS (D). HFHF diet as well as LPS induced an obvious dilatation of Bowman's space (arrowheads), hyaline casts (H), inflammatory cells infiltrations (bifid arrow), and dilatation of the renal tubules (D) and the blood vessels (C). The tubular epithelium showed multiple degenerated cells with cytoplasmic vacuolation and pyknotic nuclei (arrows). E-G) Vitamin E almost preserved the normal architecture of the kidney. Data are expressed as mean ± SEM. $ p<0.05 vs ConD-V, ! p<0.05 vs ConD-E, @ p<0.05 vs respective vitamin E treated group, % p<0.05 vs ConD-LPS, # p<0.05 vs HFHF-LPS.*

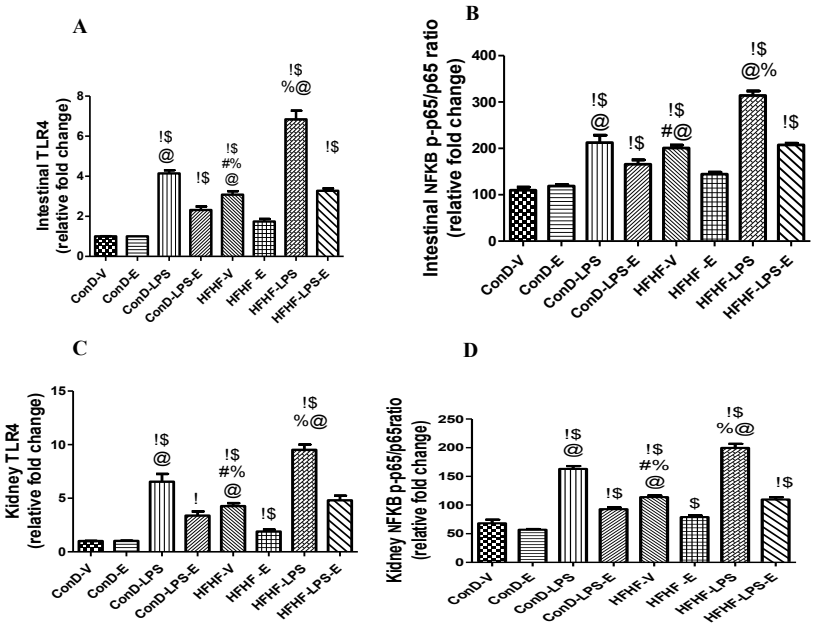

Fig. 4. *A high-fat high fructose diet upregulated toll-like receptor 4 (TLR4) and enhanced endotoxin-induced nuclear factor kappa B (NFkB) expression in renal and intestinal tissues and vitamin E reversed the effects. ConD: control diet; HFHF: High-fat-High-Fructose diet; LPS: lipopolysaccharide; E: vitamin E; V: vehicle. Data are expressed as mean ± SEM. $ p<0.05 vs ConD-V, ! p<0.05 vs ConD-E, @ p<0.05 vs respective vitamin E treated group, % p<0.05 vs ConD-LPS, # p<0.05 vs HFHF-LPS.*

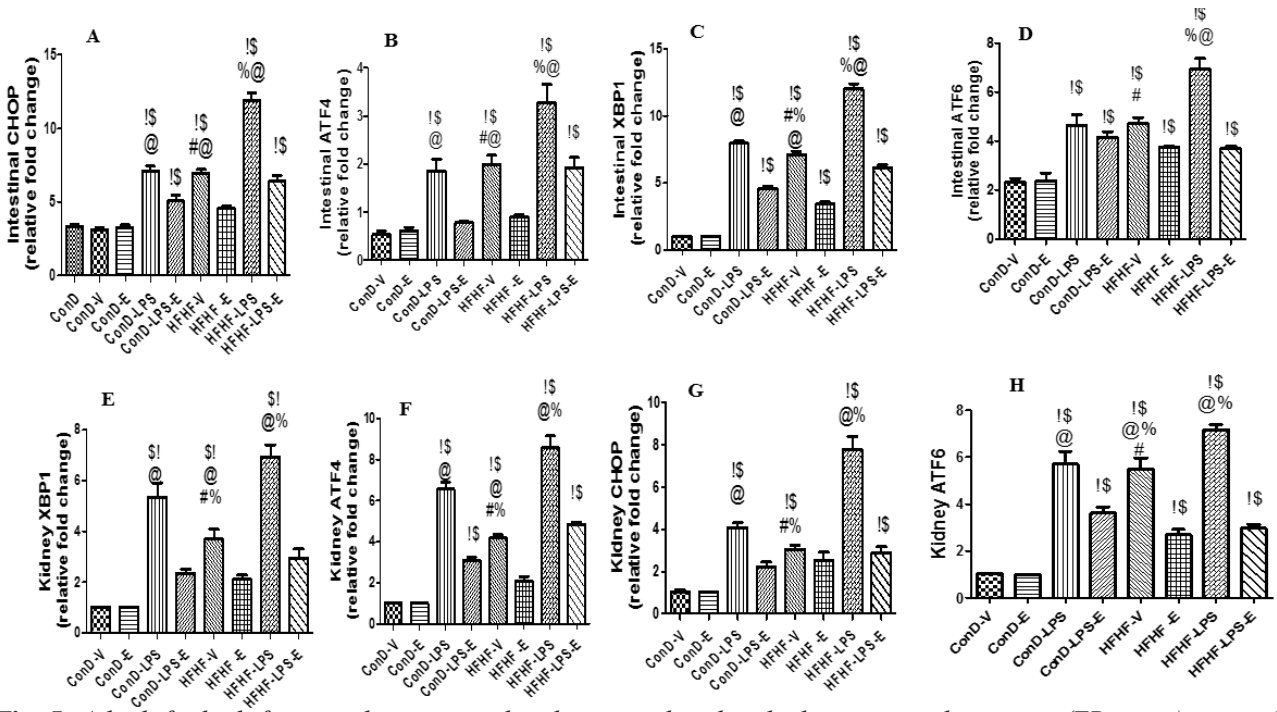

Fig. 5. *A high-fat high fructose diet promoted endotoxin-induced endoplasmic reticulum stress (ER stress) in renal and intestinal tissues and vitamin E reversed the effects. Intestinal (A-D) and renal (E-H) tissues RT-PCR analysis for XBP-1 (A&F), ATF4 (B&G), CHOP (C& H), and ATF6 (E&I) mRNA relative expression normalized to the beta-actin housekeeping gene from rats fed on control diet (ConD) or high-fat high fructose (HFHF) diets (with and without vitamin E) and subjected to LPS or vehicle (V). Data are expressed as mean ± SEM. $ p<0.05 vs ConD-V, ! p<0.05 vs ConD-E, @ p<0.05 vs respective vitamin E treated group, % p<0.05 vs ConD-LPS, # p<0.05 vs HFHF-LPS.*

in renal and intestinal tissues in ConD-LPS, HFHF and HFHF-LPS, as illustrated in Fig. 5.

***HFHF* acted synergistically with LPS to upregulate mTOR and downregulate autophagy** *in intestinal and renal tissues and vitamin E reversed the effects of HFHF and LPS*

Consistent with an increased ER stress, the results showed a significant upregulation ($p<0.05$) of mTOR and downregulation ($p<0.05$) of the autophagy response (beclin 1, LC3, LAMP, and VMAP) in ConD-LPS, HFHF, and HFHF-LPS. Levels of previous parameters were significantly altered ($p<0.05$) in the rats with combined LPS and HFHF. However, vitamin E significantly decreased ($p<0.05$) the ER stress and augmented ($p<0.05$) the autophagy in ConD-LPS, HFHF, and HFHF-LPS, as illustrated in Fig. 6.

DISCUSSION

A high-fat high fructose diet (HFHF, western diet) induced renal priming of the immune response (TLR4 and NFKB) and aggravated the inflammatory response to LPS. The previous findings could be attributed to a change in Bacteroid/Firmicutes ratio (dysbiosis) and elevated serum levels of SCFA and LPS. The data also suggest that the primed inflammatory response could be possibly due to persistent upregulation of ER stress responses (ATF6/CHOP/XBP1). The results indicate also that downregulation of autophagy (beclin 1, LC3, Vamp8, and LAMP) and upregulation of caspase 12 rendered intestinal and renal cells vulnerable to ER stress. Moreover, downregulation of autophagy could be involved in the intestinal barrier and proximal tubular renal injuries. Vitamin E supplementation dampened

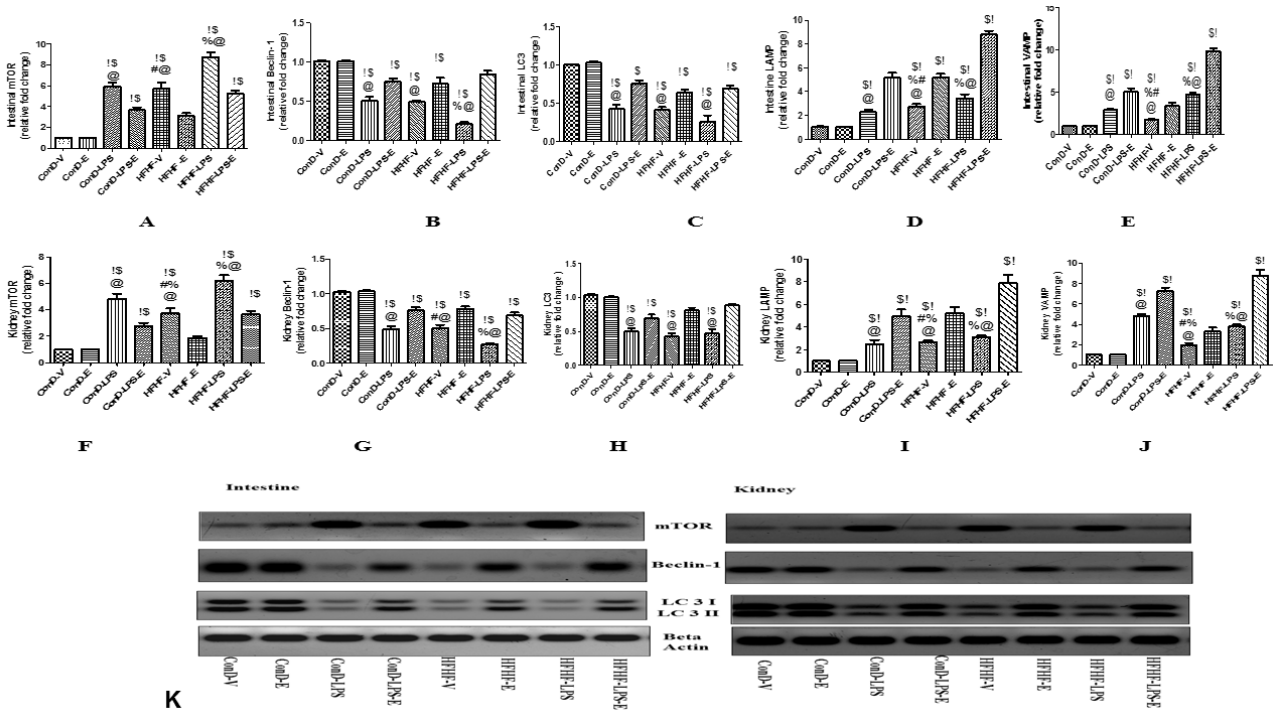

Fig. 6. *A high-fat high fructose diet and lipopolysaccharide acted synergistically to dampen the autophagy-related markers in renal and intestinal tissues and vitamin E reversed the effects. Intestinal (A-E) and renal (F-J) tissues RT-PCR and western blot analysis for Mtor (A & F), beclin-1 (B & G), LC 3 (C & H), LAMP (D &I), and VAMP (E & J) mRNA relative expression normalized to the beta-actin housekeeping gene from rats fed on a control diet (ConD) or high-fat high fructose (HFHF) diets (with and without vitamin E) and subjected to LPS or vehicle (V). (K) Western blot indicated protein expression of mTOR, beclin-1, and LC3 . Data are expressed as mean ± SEM. $ $p<0.05$ vs ConD-V, ! $p<0.05$ vs ConD-E, @ $p<0.05$ vs respective vitamin E treated group, % $p<0.05$ vs ConD-LPS, # $p<0.05$ vs HFHF-LPS.*

Table III. *Impact of high fat-high fructose (HFHF), lipopolysaccharide (LPS), and vitamin E on renal function and structure*

	ConD-V	ConD-E	ConD-LPS	ConD-LPS-E	HFHF-V	HFHF -E	HFHF-LPS	HFHF-LPS-E
KWI	0.7±0.0	0.9±0.1	1.4±0.3	1.3±0.1	1.1±0.3	0.9±0.1	1.1±0.2	1.1±0.2
Creatinine (mg/dl)	0.2 ± 0.0	0.1 ± 0.0	1.1 ± 0.3$^{!\$@}$	0.4 ± 0.2	0.7 ± 0.2$^{!\$@\#\%}$	0.3 ± 0.0	1.8 ± 0.2$^{!\$@\%}$	0.6±0.1$^{\$}$
BUN (mg/dl)	34.8±14.2	34.7±5.9	80.7±9.7$^{!\$@}$	51.8±8.4	74.6±12.9$^{!\$@\#}$	42.4±4.4	112.2±4.9$^{\$!@\%}$	76.9±17.5$^{\$}$
Cr clearance (ml/min/kg)	37.3±40.9	38.6±20.7	1.0±0.9$^{!\$@}$	25.6±19.4	2.2 ±2.0$^{\$\ @\#}$	11.4±12.9	0.7±0.6$^{\$@\%}$	5.7±1.3
NGAL (ng/ml)	0.4±0.2	0.5±0.1	1.9±0.6$^{!\$@}$	0.9±0.0	1.0±0.2 $^{\#\%@}$	0.6±0.1	2.8±0.5$^{\$@\%}$	1.1±0.2
Renal Injury Score	0.6±0.3	0.6±0.3	3.7±0.1$^{!\$@}$	1.0±0.3	2.5±0.2 $^{\$@\%\#}$	0.5±0.2	4.5±0.2$^{\$@\%}$	0.8±0.3
MBP (mmHg)	85±7.5	73±1.8	80±5.1	96±12.0	117±3$^{\$!}$	111±10.3$^{\$!}$	113±11.0$^{\$!}$	104±7.2$^{\$!}$

Data are expressed as mean ± SD. ConD: control diet; LPS: lipopolysaccharide; HFHF: high fat-high fructose; KWI: Kidney weight index; BUN: Blood urea nitrogen; Cr clearance: creatinine clearance; NGAL: neutrophil gelatinase-associated lipocalin; MBP: mean blood pressure. ! P< 0.05 vs ConD-V ; $P< 0.05 vs ConD-E; # P< 0.05 vs HFHF-LPS; @ P< 0.05 vs the corresponding group treated with vitamin E and % P< 0.05 vs ConD-LPS

Table IV. *Relationship between* ***serum LPS and SCFA and*** *biochemical and* **morphological** *changes in kidney*

	Biochemical & morphological parameters	**Pearson's correlationship**	
		r	*P*
LPS	**Creatinine**	0.85	< 0.0001
	CCr	-0.49	0.0006
	NGAL	0.88	< 0.0001
	Renal score injury	0.56	< 0.0001
SCFA	**Creatinine**	0.78	< 0.0001
	CCr	-0.43	0.0032
	NGAL	0.66	< 0.0001
	Renal score injury	0.70	< 0.0001

LPS: lipopolysaccharide; SCFA: short-chain fatty acids; CCr: creatinine clearance; NGAL: neutrophil gelatinase-associated lipocalin

ER stress, enhanced autophagy, and ameliorated the inflammatory response.

In this study, HFHF-induced dysbiosis (decreased Bacteroides and increased firmicutes) was observed to provoke the intestinal leakage leading to a systemic release of LPS and SCFAs (short-chain fatty acids produced by fermentation of undigested carbohydrates via intestinal microbiota). The relationship between microbiota composition and the circulating levels of SCFAs and LPS was previously reported (25, 26). High levels of serum LPS and SCFAs could affect other distant organs (27-29). Concurrently, we found that chronic intake of HFHF acts synergistically with injected endotoxin to increase systemic LPS and SCFAs secretions, and to induce TLR4 and NFKB expressions in the renal tissue. Our data revealed also that serum levels of LPS and SCAFs were strongly related to the observed renal alterations.

Based on the emerging evidence, the inflammatory response is commonly triggered as a result of ER stress. In intestinal and renal tissues, we found that the increased TLR4 and NFKB expressions in parallel accompanied by upregulation of ER stress (ATF6/CHOP/XBP1), and these findings are inconsistent with previous studies (30, 31). Recent data revealed that NFKB activation is linked to ER stress activation in the liver (32) and adipose tissue (33). This finding coincides with a significant decrease in the IL-1β level after LPS injection in CHOP-/-mice, signifying that inhibition of ER stress reduces inflammation. Inflammation activates a positive feedback mechanism involving ER stress to induce pro-inflammatory cytokine release leading to a vicious cycle (34, 35).

In this study, upregulation of caspase 12 simultaneously with ER stress biomarkers supports the strong relationship between ER-stress and apoptotic pathways. ER stress could be invoked to explain caspase upregulation in renal and intestinal tissues. Sustained ER stress stimulates several pro-apoptotic events leading to apoptosis. ATF4/ATF6-CHOP axis activation was found to stimulate caspase 12 in parallel with inhibition of anti-apoptotic proteins of the Bcl-2 family (36). Moreover, cells were found to resist apoptosis in CHOP knockout mice (37). In atherosclerosis, suppression of the ER stress was found to reduce apoptosis of endothelial cells (38).

Maintaining basal levels of autophagic activity is crucial for cell survival. Consistent with previous results (39-42), we found that dampening of autophagy is accompanied by a reduced expression of both occludin and ZO-1 and enhanced renal tubular injury. We proposed that inhibition of autophagy contributes to prolonged ER stress after HFHF and LPS. Autophagy and endoplasmic reticulum may work independently or synergistically to relieve stress and protect cells, but they could induce cell death with extreme stress (43). In chronic neurodegenerative diseases, sustained ER stress frequently causes activation of the autophagic pathway to alleviate ER stress; however, impaired autophagy leads to inefficient clearance of the accumulated proteins (44). Prolonged ER stress inhibits autophagy via activation of the ER-resident protein RTN3, which enhances the interaction between beclin1 and Bcl-2 (45). Furthermore, ER stress-induced autophagy inhibition may be mediated by NFKB activation (46). Growing evidence implicates NFKB in autophagy inhibition through the activation of mTOR (47, 48). Synergistic effects of HFHF and LPS on the ER stress response support the role of the insult strength on the degree of ER stimulation and the ability of autophagy to attenuate ER stress (49).

Vitamin E was found to protect cells against oxidative stress and display anti-inflammatory properties. We found that vitamin E could ameliorate the effects of HFHF on the kidney by reducing the release of LPS and SCFA. Vitamin E restored the disruption of the barrier function of the intestine, a result similar to few other studies (13, 50-52). Similarly to Nighot and Ma (40), we found that vitamin E alleviated the decrease of occludin and ZO-1 expressions. Furthermore, we found that concomitant intake of vitamin E restored intestinal bacterial homeostasis. This means that part of the impact of vitamin E on the intestinal wall could be due to the gut microbiota's community changes. Previous findings are further supported by a study conducted in pregnant women, which showed that higher intake of vitamin E was associated with a decrease in Firmicutes and an increase in Bacteroides (53).

Vitamin E can influence intestinal and renal cell viability through modulating ER stress in parallel with the autophagy pathway. Our data, consistent with previous reports on various cancer cells (54-56), indicate that vitamin E may induce autophagy and dampen ER stress. Vitamin E is a strong inducer of autophagy via Akt/AMPK/mTOR signaling (57-58). Previous effects of vitamin E on the expression of ER stress markers could explain its ability to ameliorate inflammation and enhance autophagy (16, 59, 60).

Our findings suggest that the western diet persistently increased serum concentrations of LPS and SCFA to induce priming of the immune response in the renal tissue. There is a cross-talk between the NFKB pathway, ER stress, apoptosis, and autophagy that determines the fates of intestinal and renal cells. Vitamin E supplementation restores intestinal junction integrity and protects the kidney via suppression of ER stress and enhancement of autophagy. Our results are interesting as they provide a mechanistic explanation for diet style being an independent risk factor for renal disease progression.

ACKNOWLEDGEMENTS

The authors would like to thank Afaf Ahmed and Tarek Mamdouh for their skilful technical assistance. This study was supported by the Cairo University Research Funds

REFERENCES

1. Zhang J, Ankawi G, Sun J, Digvijay K, Yin Y, Rosner MH, Ronco C. Gut-kidney crosstalk in septic acute kidney injury. Crit. Care 2018; 22(1):117.
2. Delbrel E, Soumare A, Naguez A, et al. HIF-1α triggers ER stress and CHOP-mediated apoptosis in alveolar epithelial cells, a key event in pulmonary fibrosis. Sci Rep 2018; 8(1):17939.
3. Zhou L, Tan J hui, Cao R chang, et al. ATF6 regulates the development of chronic pancreatitis by inducing p53-mediated apoptosis. Cell Death Dis 2019; 10(9):662.
4. Tan JH, Cao RC, Zhou L, et al. ATF6 aggravates acinar cell apoptosis and injury by regulating p53/AIFM2 transcription in severe acute pancreatitis. Theranostics 2020; 10(18):8298-314.
5. Aslani MR, Ghobadi H, Panahpour H, Ahmadi M, Khaksar M, Heidarzadeh M. Modification of lung endoplasmic reticulum genes expression and NF-kB protein levels in obese ovalbumin-sensitized male and female rats. Life Sci 2020; 247:117446.
6. Kumar A, Singh PK, Zhang K, Kumar A. Toll-like receptor 2 (TLR2) engages endoplasmic reticulum stress sensor IRE1α to regulate retinal innate responses in Staphylococcus aureus endophthalmitis. FASEB J 2020; 34(10):13826-38.
7. Stengel S, Fazio A, Lipinski S, et al. Activating Transcription Factor 6 mediates inflammatory signals in intestinal epithelial cells upon endoplasmic reticulum stress. Gastroenterology 2020; 159(4):1357-74.
8. Zhao D, Du L-L. Epr1, a UPR-upregulated soluble autophagy receptor for reticulophagy. Autophagy 2020; 16(11):2112-3.
9. Yin J, Gu L, Wang Y, Fan N, Ma Y, Peng Y. Rapamycin improves palmitate-induced ER stress/NF B pathways associated with stimulating autophagy in adipocytes. Mediators Inflamm 2015; 2015:272313.
10. Yang L, Li P, Fu S, Calay ES, Hotamisligil GS. Defective hepatic autophagy in obesity promotes ER stress and causes insulin resistance. Cell Metab 2010; 11(6):467-78.
11. Zhou X, Fouda S, Li D, Zhang K, Ye J-M. Involvement of the Autophagy-ER stress axis in high fat/carbohydrate diet-induced nonalcoholic fatty liver disease. Nutrients 2020; 12(9):2626.
12. Montagnani Marelli M, Marzagalli M, et al. Vitamin E δ-tocotrienol triggers endoplasmic reticulum stress-mediated apoptosis in human melanoma cells. Sci Rep 2016; 6(1):30502.
13. Tahan G, Aytac E, Aytekin H, et al. Vitamin E has a dual effect of anti-inflammatory and antioxidant activities in acetic acid-induced ulcerative colitis in rats. Can J Surg 2011; 54(5):333-8.
14. Bozaykut P, Ekren R, Sezerman OU, Gladyshev VN, Ozer NK. High-throughput profiling reveals perturbation of endoplasmic reticulum stress-related genes in atherosclerosis induced by high-cholesterol diet and the protective role of vitamin E. BioFactors 2020; 46(4):653-64.
15. Karabulut-Bulan O, Bolkent S, Yanardag R, Bilgin-Sokmen B. The role of vitamin C, vitamin E, and selenium on cadmium-induced renal toxicity of

rats. Drug Chem Toxicol 2008; 31(4):413-26.
16. Xu C, Sun R, Qiao X, Xu C, Shang X, Niu W, Chao Y. Effect of vitamin e supplementation on intestinal barrier function in rats exposed to high altitude hypoxia environment. Korean J Physiol Pharmacol 2014; 18(4):313-20.
17. Liu X, Lu J, Liao Y, et al. Dihydroartemisinin attenuates lipopolysaccharide-induced acute kidney injury by inhibiting inflammation and oxidative stress. Biomed Pharmacother 2019; 117:109070.
18. Sabry MM, Ahmed MM, Maksoud OMA, et al. Carnitine, apelin and resveratrol regulate mitochondrial quality control (QC) related proteins and ameliorate acute kidney injury: role of hydrogen peroxide. Arch Physiol Biochem 2020; 13:1-10.
19. Hamzawy M, Gouda SAA, Rashid L, Attia Morcos M, Shoukry H, Sharawy N. The cellular selection between apoptosis and autophagy: roles of vitamin D, glucose and immune response in diabetic nephropathy. Endocrine 2017; 58(1):66–80.
20. Han M, Li Y, Liu M, Li Y, Cong B. Renal neutrophil gelatinase associated lipocalin expression in lipopolysaccharide-induced acute kidney injury in the rat. BMC Nephrol 2012; 13(1):25.
21. Kristensen NB. Quantification of whole blood Short-chain fatty acids by gas chromatographic determination of plasma 2-chloroethyl derivatives and correction for dilution space in erythrocytes. Acta Agric Scand A Anim Sci 2000; 50(4):231-6.
22. Niibo M, Shirouchi B, Umegatani M, et al. Probiotic Lactobacillus gasseri SBT2055 improves insulin secretion in a diabetic rat model. J Dairy Sci 2019; 102(2):997-1006.
23. Chen Y, Jin S, Teng X, et al. Hydrogen sulfide attenuates LPS-induced acute kidney injury by inhibiting inflammation and oxidative stress. Oxid Med Cell Longev 2018; 2018:6717212.
24. Erben U, Loddenkemper C, Doerfel K, et al. A guide to histomorphological evaluation of intestinal inflammation in mouse models. Int J Clin Exp Pathol 2014; 7(8):4557-76.
25. Ban-Tokuda T, Maekawa S, Miwa T, Ohkawara S, Matsui H. Changes in faecal bacteria during fattening in finishing swine. Anaerobe 2017; 47:188-93.
26. Lobo LA, Benjamim CF, Oliveira AC. The interplay between microbiota and inflammation: lessons from peritonitis and sepsis. Clin Transl Immunol 2016; 5(7):e90.
27. Singh V, Yeoh BS, Chassaing B, et al. Dysregulated microbial fermentation of soluble fiber induces cholestatic liver cancer. Cell 2018; 175(3):679-94.e22.
28. Park J, Goergen CJ, HogenEsch H, Kim CH. Chronically elevated levels of short-chain fatty acids induce T cell-mediated ureteritis and hydronephrosis. J Immunol 2016; 196(5):2388-400.
29. Wieland A, Frank DN, Harnke B, Bambha K. Systematic review: microbial dysbiosis and nonalcoholic fatty liver disease. Aliment Pharmacol Ther 2015; 42(9):1051-63.
30. Schmitz M, Shaban M, Albert B, Gökçen A, Kracht M. The crosstalk of endoplasmic reticulum (ER) stress pathways with NF-κB: Complex mechanisms relevant for cancer, inflammation and infection. Biomedicines 2018; 6(2):58.
31. Kilberg MS, Balasubramanian M, Fu L, Shan J. The transcription factor network associated with the amino acid response in mammalian cells. Adv Nutr 2012; 3(3):295-306.
32. Zhao M, Zang B, Cheng M, Ma Y, Yang Y, Yang N. Differential responses of hepatic endoplasmic reticulum stress and inflammation in diet-induced obese rats with high-fat diet rich in lard oil or soybean oil. PLoS One 2013; 8(11).
33. Garfinkel BP, Hotamisligil GS. ER stress promotes inflammation through Re-wIREd macrophages in obesity. Mol. Cell 2017; 66(6):731-3.
34. Kim S, Joe Y, Surh Y-J, Chung HT. Differential regulation of Toll-like receptor-mediated cytokine production by unfolded protein response. Oxid Med Cell Longev 2018; 2018:9827312.
35. Masson GS, Nair AR, Dange RB, Silva-Soares PP, Michelini LC, Francis J. Toll-Like Receptor 4 promotes autonomic dysfunction, inflammation and microglia activation in the hypothalamic paraventricular nucleus: role of endoplasmic reticulum stress. PLoS One 2015; 10(3):e0122850.
36. Schönthal AH. Endoplasmic reticulum stress: its role in disease and novel prospects for therapy. Scientifica (Cairo) 2012; 2012:1-26.
37. Jung SY, Kim SS, Yeo SG. Impact of endoplasmic reticulum stress in otorhinolaryngologic diseases. Int J Mol Sci 2020; 21(11):1-23.

38. Kim S, Woo CH. Laminar flow inhibits ER stress-induced endothelial apoptosis through PI3K/Akt-dependent signaling pathway. Mol Cells 2018; 41(11):964-70.
39. Wong M, Ganapathy AS, Suchanec E, Laidler L, Ma T, Nighot P. Intestinal epithelial tight junction barrier regulation by autophagy-related protein ATG6/beclin 1. Am J Physiol Physiol 2019; 316(5):C753-65.
40. Nighot P, Ma T. Role of autophagy in the regulation of epithelial cell junctions. Tissue barriers 2016; 4(3):e1171284.
41. Sunahara S, Watanabe E, Hatano M, et al. Influence of autophagy on acute kidney injury in a murine cecal ligation and puncture sepsis model. Sci Rep 2018; 8(1):1050.
42. Hsiao HW, Tsai KL, Wang LF, Chen YH, Chiang PC, Chuang SM, Hsu C. The decline of autophagy contributes to proximal tubular dysfunction during sepsis. Shock 2012; 37(3):289-96.
43. Cybulsky A V. Endoplasmic reticulum stress, the unfolded protein response and autophagy in kidney diseases. Nat Rev Nephrol 2017; 13(11):681-96.
44. Cai Y, Arikkath J, Yang L, Guo ML, Periyasamy P, Buch S. Interplay of endoplasmic reticulum stress and autophagy in neurodegenerative disorders [Internet]. Autophagy. 2016; 12(2):225-44.
45. Wilkinson S. Emerging Principles of Selective ER Autophagy. J. Mol. Biol 2020; 432(1):185-205.
46. Zhu X, Huang L, Gong J, et al. NF-κB pathway link with ER stress-induced autophagy and apoptosis in cervical tumor cells. Cell Death Discov 2017; 3:17059.
47. Trocoli A, Djavaheri-Mergny M. The complex interplay between autophagy and NF-κB signaling pathways in cancer cells. Am J Cancer Res 2011; 1(5):629-49.
48. Dhingra R, Gang H, Wang Y, et al. Bidirectional regulation of nuclear factor-κB and mammalian target of rapamycin signaling functionally links Bnip3 gene repression and cell survival of ventricular myocytes. Circ Heart Fail 2013; 6(2):335-43.
49. Luchetti F, Crinelli R, Cesarini E, et al. Endothelial cells, endoplasmic reticulum stress and oxysterols. Redox Biol 2017; 13:581-7.
50. Liu F, Cottrell JJ, Furness JB, et al. Selenium and vitamin E together improve intestinal epithelial barrier function and alleviate oxidative stress in heat-stressed pigs. Exp Physiol 2016; 101(7):801-10.
51. Li L, Krause L, Somerset S. Associations between micronutrient intakes and gut microbiota in a group of adults with cystic fibrosis. Clin Nutr 2017; 36(4):1097-104.
52. Pierre JF, Hinterleitner R, Bouziat R, et al. Dietary antioxidant micronutrients alter mucosal inflammatory risk in a murine model of genetic and microbial susceptibility. J Nutr Biochem 2018; 54:95-104.
53. Mandal S, Godfrey KM, McDonald D, et al. Fat and vitamin intakes during pregnancy have stronger relationships with a proinflammatory maternal microbiota than does carbohydrate intake. Microbiome 2016; 4(1):55
54. Fontana F, Moretti RM, Raimondi M, et al. δ□ Tocotrienol induces apoptosis, involving endoplasmic reticulum stress and autophagy, and paraptosis in prostate cancer cells. Cell Prolif 2019; 52(3):e12576.
55. Comitato R, Guantario B, Leoni G, Nesaretnam K, Ronci MB, Canali R, Virgili F. Tocotrienols induce endoplasmic reticulum stress and apoptosis in cervical cancer cells. Genes Nutr 2016; 11:32.
56. Tiwari R V., Parajuli P, Sylvester PW. γ-Tocotrienol-induced endoplasmic reticulum stress and autophagy act concurrently to promote breast cancer cell death. Biochem Cell Biol 2015; 93(4):306-20.
57. Yu Y, Hou L, Song H, Xu P, Sun Y, Wu K. Akt/AMPK/mTOR pathway was involved in the autophagy induced by vitamin E succinate in human gastric cancer SGC-7901 cells. Mol Cell Biochem 2017; 424(1-2):173-83.
58. Yang P, Zhao J, Hou L, Yang L, Wu K, Zhang L. Vitamin E succinate induces apoptosis via the PI3K/AKT signaling pathways in EC109 esophageal cancer cells. Mol Med Rep 2016; 14(2):1531-7.
59. Ilçe F, Gök G, Pandir D. Acute effects of lipopolysaccharide (LPS) in kidney of rats and preventive role of vitamin E and sodium selenite. Hum Exp Toxicol 2019; 38(5):547-60
60. Jiang Q. Natural forms of vitamin E: metabolism, antioxidant, and anti-inflammatory activities and their role in disease prevention and therapy. Free Radic Biol Med 2014; 72:76-90.